ACADEMIC PRESS

Available online at www.sciencedirect.com
SCIENCE DIRECT®

Journal of Catalysis 219 (2003) 231–241

JOURNAL OF CATALYSIS

www.elsevier.com/locate/jcat

# Factors determining the suitability of zeolite BEA as *para*-selective nitration catalyst

Samantha Bernasconi, Gerhard D. Pirngruber, Andreas Kogelbauer,[1] and Roel Prins *

*Institute for Chemical and Bioengineering, Swiss Federal Institute of Technology (ETH), CH-8093 Zurich, Switzerland*

Received 23 January 2003; revised 16 April 2003; accepted 16 April 2003

**Abstract**

The nitration of toluene and 2-nitrotoluene with acetyl nitrate was investigated using several solid acid catalysts. In the nitration of toluene, enhanced *para*-selectivity was observed only with zeolite BEA. For the nitration of 2-nitrotoluene, all the catalysts displayed good *para*-selectivity, but only BEA led to high yields. The superior performance of BEA was due to the fact that only with this zeolite did the heterogeneously catalyzed reaction compete successfully with the homogeneous nitration in the liquid phase. Geometrical considerations showed that the high *para*-selectivity of BEA was not caused by classical transition-state selectivity but was induced by the reaction of the arene with a surface-bound acetyl nitrate complex. The existence of this complex was supported by NMR measurements, which showed that its formation is a specific property of zeolite BEA.


*Keywords:* Nitration; Acetyl nitrate; BEA; Toluene; Nitrotoluene; Dinitrotoluene; *para*-selectivity; NMR

## 1. Introduction

The nitration of aromatics is one of the oldest and most important processes in the chemical industry for the production of intermediates. Extensive and well-documented reviews have been published about the mechanism and general nitration systems as well as about nitration with heterogeneous catalysts [1–5]. The typical product composition obtained in the industrially applied mixed-acid nitration of toluene and nitrotoluene (NT) shows an excess of the less desirable *ortho*-substituted products. Being an irreversible reaction, nitration does not permit a shift in the product composition by reequilibration of the products [6]. Because of the higher commercial value of the *para*-products a *para*-selective nitration reaction is desirable.

Several studies reported attempts to shift the product composition in favor of the *para*-substituted products, 4-nitrotoluene (4-NT) and 2,4-dinitrotoluene (2,4-DNT), with solid acids as catalysts. For the most part, zeolites such as mordenite [7–10], ZSM-5 [7,8,10,11], ZSM-11 [12], beta [7,8,10,13], and Y [8–10,12] have been tested as catalysts in different nitration systems and have led to good *para*-selectivities. Clay-supported metal nitrates [14,15] as well as $SiO_2$ and $Al_2O_3$ impregnated with $H_2SO_4$ and $H_3PO_4$ [16] have been investigated. Our previous work has shown that, in the liquid-phase nitration with 65 wt% nitric acid as a nitrating agent at ambient temperature, zeolites are poor catalysts because of the overwhelming mediating effect of water on the acidity of zeolites [17]. The majority of studies tried to overcome this by applying organic nitrating agents such as various acetyl nitrates [12,13] or alkyl nitrates [7,11]. Some studies on nitrogen dioxide (dinitrogen tetroxide) [7,18] and dinitrogen pentoxide [9] have been carried out, and nitric acid in combination with water-tolerant catalysts or in reaction regimes other than the liquid phase has also been reported [10,12,16,19,20]. Thus far, nitric acid-based systems have shown comparably low activity in combination with reaction distillation, and nitration systems that are not based on nitric acid are hardly viable alternatives to large-scale application.

The use of zeolites seems to be the most promising route to obtain *para*-selective nitration and the concept of shape selectivity has been commonly invoked to explain the enhanced *para*-selectivity [10–12]. Of particular inter-

* Corresponding author.
*E-mail address:* prins@tech.chem.ethz.ch (R. Prins).
[1] Present address: Department of Chemical Engineering and Chemical Technology, Imperial College of Science, Technology and Medicine, London SW7 2BY, UK.

0021-9517/$ – see front matter 
doi:10.1016/S0021-9517(03)00201-X

est is the high regioselectivity obtained with zeolite beta and nitric acid/acetic anhydride reported initially by Smith et al. [13,21]. Beta, having 12-membered ring channels is not expected to induce shape selectivity in its classical sense [6]. NMR studies suggested that the high *para*-selectivity of zeolite beta might be linked to steric hindrance of the *ortho*-position, induced by adsorption, rather than to classical transition-state selectivity [22].

In the present work we concentrate on the nitration with a broad variety of beta zeolites with different characteristics. The aim was to elucidate the reason for he exceptionally high selectivity observed exclusively with beta zeolites. For the sake of comparison other zeolites and solid acids were also tested.

## 2. Experimental

### *2.1. Catalysts*

A variety of commercially available beta zeolites as well as beta synthesized in our laboratory were used in this study. PB1, PB3, PB5, and PB13 are different batches obtained from CU Chemie Uetikon AG (PB3 and PB13 were in the $Na^+$ form with template, and PB1 and PB5 were in the $Na^+$ form without template). BEA-24 ($Na^+$ form without template) and BEA-150 ($H^+$ form) were obtained from Süd-Chemie AG, PQ (in $NH_4{}^+$ form) from Zeolyst International, and RAHB and RAMB (both in $Na^+$ form with template) from the Research Institute of Petroleum Processing (RIPP) in Beijing. In the case of the $Na^+$ zeolites, the proton forms were prepared by a threefold 1 h ion exchange of the parent zeolites with a 1 M aqueous $NH_4NO_3$ solution (10 ml per 1 g zeolite) under reflux. The PQ zeolite was calcined and ion-exchanged only once. After washing with deionized water, the zeolites were dried and calcined in air at 550 °C for 8 h.

Pure silica beta was synthesized according to the procedure of Camblor et al. [23]. Tetraethoxysilane (15.59 g, Fluka) was added to a mixture of 14.87 g 40% TEAOH (Fluka) and 4.55 g of distilled water. Ethanol was evaporated by stirring the mixture at ambient temperature for 6.5 h, and 1.68 g 48% hydrofluoric acid (HF, Fluka) was added drop by drop. The obtained gel was heated in a Teflon-lined autoclave at 140 °C for 39 h and stirred at 60 rpm. The obtained zeolite (referred to as Si-Beta) was washed until the filtrate was neutral. Calcination for template removal was carried out as explained above.

Zeolite ZSM-5 (PZ-2/40) and mordenite (PM22) were purchased from CU Chemie Uetikon in the $Na^+$ form, PZ-2/40 with template. ZSM-5 was calcined and ion-exchanged in the same way as the commercial beta zeolites. Dealuminated mordenite was obtained after thermal treatment with subsequent acid leaching [24]. The $Na^+$ form was ion-exchanged once with 1 M HCl (10 ml for 1 g zeolite) at reflux temperature for 1 h and then twice with 1 M $NH_4NO_3$ (10 ml for 1 g zeolite) under the same conditions. The obtained zeolite is referred to as H-MOR(4.6). The resulting ammonium form of the zeolite was calcined at 750 °C for 2 h (heating rate: 1 °C/min) and then treated with 6 M $HNO_3$ (10 ml for 1 g zeolite) for 16 h at reflux temperature to remove the extraframework aluminum. The modified zeolite (denominated H-MOR(74)) was finally calcined in air at 500 °C for 8 h.

USY was prepared from a NaY received from CU Chemie Uetikon. NaY was subjected to a twofold ion exchange with a 1 M $NH_4NO_3$ (5 ml/g) at 90 °C for 1 h prior to each steaming treatment (6 h, 500 °C, 5 ml $H_2O$/min). The steaming treatment was repeated twice and then the sample was finally leached with 6 M $HNO_3$ (10 ml/g) at room temperature for 21 h.

ZSM-12 was synthesized according to the following procedure. To 87 g sodium silicate solution (Merck), diluted with 40.20 g distilled water, was added under vigorous stirring 17.81 g hexamethyleneimine (Fluka). The solution was stirred for 15 min. Aluminum sulfate (2.05 g, Fluka) and 7.17 g sulfuric acid, diluted in 220 g distilled water, were added drop by drop. After stirring for 2 h at ambient temperature the solution was heated in a Teflon-lined autoclave at 150 °C for 88 h and stirred at 250 rpm. The obtained zeolite was washed with water and with ethanol and then calcined at 750 °C for 6 h and subsequently ion-exchanged in the same way as the commercial beta zeolites. An attempt was made to dealuminate ZSM-12 by means of deep-bed calcination in air at 1000 °C for 5 h with subsequent acid leaching in a similar way as for mordenite.

Amberlyst-15 (Fluka) and Nafion-SAC25 (DuPont), a nafion/silica nanocomposite, were used as purchased.

### *2.2. Characterization*

The structural integrity of the zeolites after each modification was checked by X-ray diffraction on a Siemens D5000 X-ray diffractometer using Cu-$K_\alpha$ radiation. The Si and Al contents of the zeolites were determined by atomic absorption spectrometry on a Varian SpectrAA instrument after the zeolites were dissolved in HF. Nitrogen adsorption was carried out at −196 °C on a Micromeritics ASAP 2000M volumetric analyzer. The catalysts were degassed prior to analysis under vacuum at 400 °C (120 °C in case of Amberlyst 15 and 140 °C in case of Nafion-SAC25) for at least 2 h. The specific surface area was evaluated using the BET method. The external surface area is given as the difference between the BET surface area and the micropore surface area, which was determined by the *t*-plot method [25]. The average pore diameter of pores larger than 17 Å was estimated from the desorption branch of the isotherm using the BJH method [26]. TGA measurements were carried out on a Mettler Toledo TGA/SDTA851$^e$ system. The samples were heated in a stream of air (50 ml/min) at a rate of 10 °C/min from ambient temperature to 800 °C. SEM images of the samples coated with a 5-nm-thick platinum layer

were taken on a Hitachi S-900 microscope (energy of the beam: 30 keV).

Solid-state $^{27}$Al MAS NMR spectra were recorded on fully hydrated zeolite samples using a Bruker AMX400 spectrometer at a magnetic field of 9.4 T. The spectra were recorded at a resonance frequency of 104.26 MHz and a rotor-spinning rate of 10 kHz. For each spectrum, 9720 scans were acquired using a 1.1-μs pulse length (flip angle of 15°) and a relaxation delay of 2 s. Chemical shifts are given relative to a 1 M aqueous aluminum nitrate solution.

### 2.3. Catalytic tests

Acetyl nitrate, the nitrating agent, was generated in situ from 90 wt% nitric acid and acetic anhydride (Fluka). For a typical reaction experiment 35 mmol 90 wt% nitric acid and 1.0 g of dried catalyst (130 °C, overnight) were mixed and stirred at 0 °C. Acetic anhydride (53 mmol) was added to convert nitric acid into acetyl nitrate and the water present in nitric acid into acetic acid (AcOH). Thirty-five millimoles of toluene or 3.5 mmol of 2-NT then added drop by drop in order to keep the temperature below 20 °C. After addition of the substrate, the mixture was stirred at room temperature for another 30 min to 16 h. The reaction was stopped by filtering the mixture and washing the catalysts with methylene chloride. The organic products were separated by extraction with methylene chloride and analyzed by gas chromatography using a HP 5890 gas chromatograph equipped with a HP-1 fused silica capillary column and 1,3-dinitrobenzene as the integration standard.

After filtration of the catalyst the analysis of the product composition inside of the pores was carried out dissolving the zeolite in 48 wt% HF. The products were extracted with methylene chloride and analyzed by gas chromatography.

### 2.4. $^{15}$N NMR experiments

For the solid-state NMR the zeolites were treated overnight at 130 °C to remove adsorbed species. Each sample was impregnated first with 90 wt% $HNO_3$ ($^{15}$N-enriched) and then $Ac_2O$ was added to the resulting mixture. In order to keep the samples in the powder form, the loading was kept particularly low. The $HNO_3/Ac_2O$ ratio was 0.69, not taking into account the excess of $Ac_2O$ needed to react with the water contained in the acid. The measurements were carried out on a Bruker AMX 400 spectrometer at 9.40 T, which corresponds to a resonance frequency of 40.54 MHz for $^{15}$N. The spectra were collected using a 7.5 μs pulse and a recycle delay of 20 s, and 720 transients were averaged for each spectrum. Chemical shifts were referenced to $^{15}$N-labeled glycine (Cambridge Isotope Laboratories, Inc.), in which the main peak was fixed at −345.26 ppm.

## 3. Results

### 3.1. Catalysts

Table 1 lists the characteristics of the different beta zeolites used in this work. The commercial beta zeolites of Chemie Uetikon, Süd Chemie, and Zeolyst (Figs. 1 and 2) are composed of crystallites, the sizes of which are about 0.03 to 0.1 μm and have a large external surface area between 140 and 240 $m^2/g$. The Si/Al ratio of these zeolites varied from 9 to 15, with the exception of H-BEA-150 with a Si/Al ratio of 74. The synthesized pure silicon beta zeolite consists of larger crystallites (5–8 μm Si-Beta, Fig. 2). Si-Beta has the lowest surface area and the smallest micropore volume of all the beta zeolites studied. The beta samples from RIPP (H-RAMB and H-RAHB) have intermediate crystallite dimensions (0.5–0.8 μm, Fig. 2) and higher Si/Al ratios (39 and 142) than the other beta zeolites.

ZSM-5, ZSM-12, and mordenite (PM22) are characterized by smaller total and external surface areas compared to the commercial beta zeolites (Table 2 and Fig. 3). PM22 is composed of 0.5 to 1 μm crystallites that form clusters of up to 5 μm. ZSM-12 crystallites were quite homogeneous with dimensions of 2–3 μm × 0.4–0.8 μm. The thermal treatment

Table 1
Characteristics of the beta zeolites

| | Si/Al | BET surface area ($m^2/g$) | External surface area ($m^2/g$) | Pore volume ($cm^3/g$) | Average mesopore diam. (Å) | Micropore volume ($cm^3/g$) |
|---|---|---|---|---|---|---|
| H-PB1 | 15 | 722 | 221 | 0.77 | 78 | 0.21 |
| H-PB3 | 12 | 750 | 156 | 0.51 | 46 | 0.25 |
| H-PB5 | 12 | 690 | 199 | 0.90 | 102 | 0.21 |
| H-PB13 | 9 | 670 | 233 | 0.75 | 77 | 0.18 |
| H-BEA-24 | 12 | 696 | 170 | 0.65 | 74 | 0.22 |
| H-BEA-150 | 74 | 722 | 139 | 0.63 | 71 | 0.25 |
| H-PQ | 13 | 634 | 182 | 1.06 | 136 | 0.19 |
| H-PQ[a] | 30 | 631 | 167 | 1.07 | 146 | 0.19 |
| H-RAMB | 39 | 614 | 44 | 0.42 | 68 | 0.24 |
| H-RAHB | 142 | 582 | 94 | 0.63 | 94 | 0.21 |
| Si-Beta | – | 294 | 34 | 0.35 | 133 | 0.11 |

[a] After three nitration runs with subsequent calcinations at 550 °C.

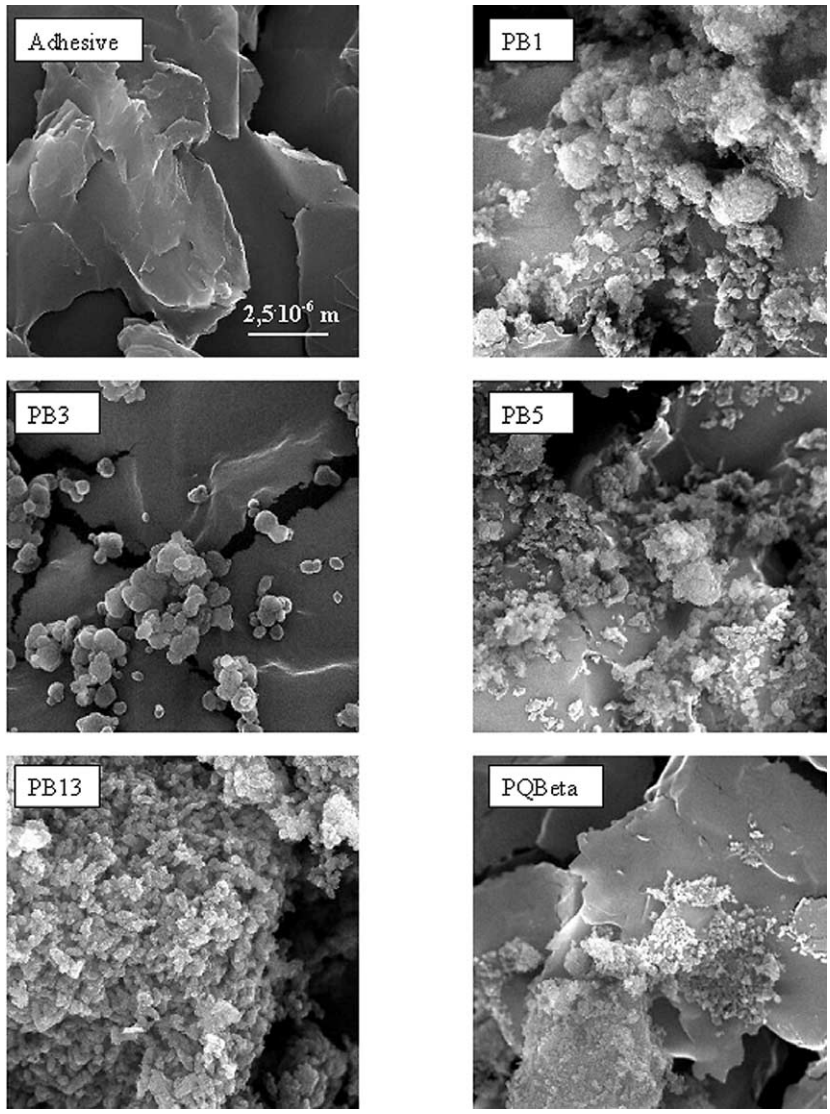


Fig. 1. SEM pictures of beta zeolites.

with subsequent acid leaching of mordenite led to a structure with a secondary mesoporous system, confirmed by the increase in the external surface area and the pore volume. The more severe thermal treatment of ZSM-12, however, had almost no effect on the characteristics of the zeolite.

### *3.2. Nitration with acetyl nitrate*

#### *3.2.1. Nitration of toluene*

Table 3 lists the results of the nitration experiments with toluene and different catalysts. A considerable amount of NT, with a product selectivity comparable to that of the mixed acid nitration, was produced even without a catalyst. This was also the case when an excess of acetic anhydride was used. A 10-fold excess of nitric acid increased the NT yield but not that of DNT. The GC analysis showed that secondary products, probably due to oxidation reactions, are present in negligible amounts, with the exception of the product of the side-chain nitration ($\alpha$-NT), which was detected in some of the nitration experiments.

Amberlyst-15 was the only catalyst that showed a noticeable DNT yield together with a slightly higher 4-NT selectivity. The activity and selectivity of the nafion/silica composite did not significantly increase compared to nafion [8], as was claimed for other reactions [27]. None of the catalysts shown in Table 3 exhibited a significantly enhanced selectivity for 4-NT. The XRD patterns of the zeolites recorded after the nitration indicated that their structural integrity was maintained.

The selectivity of the mordenite zeolite with a mesoporous system also did not show a substantial increase in 4-NT selectivity. This is in contrast to nitration in the gas phase with 65 wt% $HNO_3$, where the 4-NT-to-2-NT ratio increased from 0.7 to more than 1 in the first 2 to 3 h on stream [28].

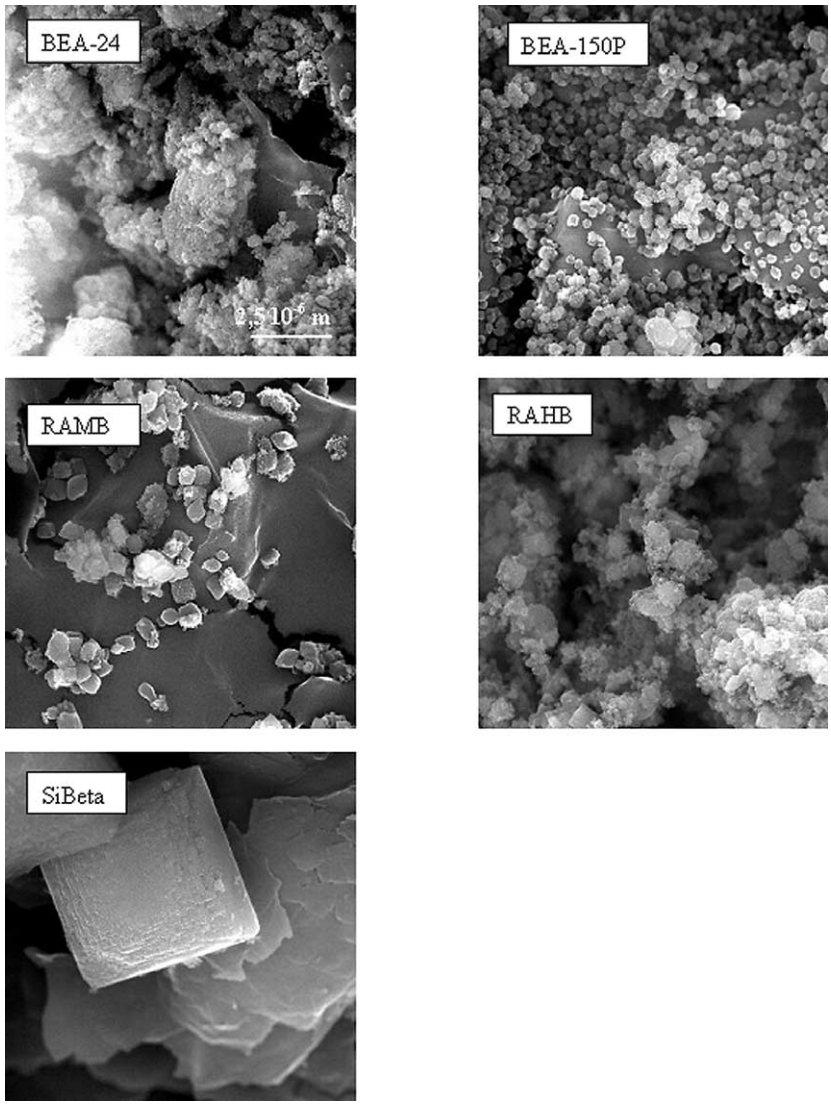


Fig. 2. SEM pictures of beta zeolites.

Most of the beta zeolites, however, exhibited an enhanced 4-NT selectivity (Table 4), as observed by Smith et al. [13,21]. Notable differences in the product selectivities were obtained depending on the beta batch used. All the commercial beta zeolites showed a higher 4-NT selectivity between 51 and 73%. The pure silicon BEA (Si-Beta), however, did not result in higher 4-NT selectivities; the beta zeolites with an intermediate crystallite size had a 4-NT selectivity between that of the micro- and the Si-beta zeolites. The Si/Al ratio did not seem to govern the selectivity. For in-

Table 2
Characteristics of other zeolites and solid acids

| | Si/Al | BET surface area ($m^2/g$) | External surface area ($m^2/g$) | Pore volume ($cm^3/g$) | Average mesopore diam. (Å) | Micropore volume ($cm^3/g$) |
|---|---|---|---|---|---|---|
| H-ZSM-5 | 19 | 408 | 44 | 0.47 | 102 | 0.16 |
| H-ZSM-12 | 47 | 250 | 12 | 0.15 | 52 | 0.10 |
| H-ZSM-12[a] | 42 | 259 | 13 | 0.16 | 55 | 0.10 |
| USY | 36 | 672 | 34 | 0.38 | 22 | 0.33 |
| H-MOR(4.6) | 4.6 | 529 | 7 | 0.26 | 61 | 0.22 |
| H-MOR(74) | 74 | 556 | 36 | 0.32 | 52 | 0.22 |
| Amberlyst-15 | – | 41 | 21 | 0.36 | 246 | 0.01 |
| Nafion-SAC25 | – | 78 | 50 | 0.51 | 202 | 0.01 |

[a] After thermal treatment at 1000 °C and acid leaching with 6 M $HNO_3$.

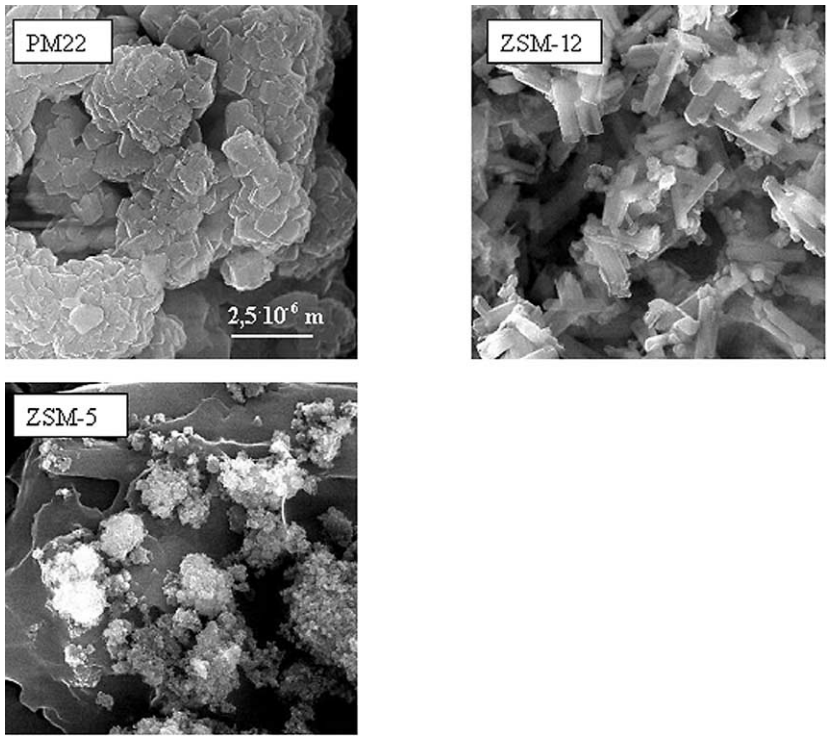


Fig. 3. SEM pictures of mordenite, ZSM-12, and ZSM-5.

Table 3
Nitration of toluene using different catalysts (90 wt% $HNO_3$, $Ac_2O$, toluene/$HNO_3 = 1$, 30 min)

| | NT yield (mol%) | DNT yield (mol%) | $S_{2\text{-NT}}$[c] (mol%) | $S_{4\text{-NT}}$[c] (mol%) |
|---|---|---|---|---|
| Blank | 76 | 0.0 | 59 | 38 |
| Blank[a] | 91 | 0.0 | 60 | 37 |
| Blank[b] | 82 | 0.0 | 60 | 37 |
| Amberlyst-15 | 74 | 2.8 | 55 | 42 |
| Nafion-SAC25 | 84 | 0.0 | 58 | 40 |
| H-ZSM-5 | 81 | 0.04 | 58 | 40 |
| H-ZSM-12 | 78 | 0.01 | 61 | 37 |
| USY | 77 | 0.0 | 59 | 38 |
| H-MOR(4.6) | 78 | 0.0 | 58 | 39 |
| H-MOR(74) | 82 | 0.04 | 57 | 43 |

[a] Toluene/$HNO_3 = 0.1$.
[b] Double molar amount of acetic acid anhydride was used.
[c] $S$ is defined as (2-NT/$\Sigma$NT) $*$ 100 and (4-NT/$\Sigma$NT) $*$ 100.

stance, H-BEA-150, with a Si/Al ratio of 74, exhibited the highest 4-NT selectivity, and beta zeolites with clearly different Si/Al ratios (H-RAMB, H-PB1, and H-PB13) gave similar 4-NT selectivities. Beta zeolites also gave a small yield of DNT, which seemed to be correlated with the enhancement in the *para*-selectivity. Table 5 shows the results of the nitration reaction with H-PB5 with varying reaction time and a toluene-$HNO_3$ ratio of 0.1. Longer reaction times led to an increase in the DNT yield and a decrease in the NT yield, in line with the sequential nature of DNT formation from NT. This was accompanied by an apparent increase in the 3-NT and 4-NT selectivities and a decrease in the 2-NT

Table 4
Nitration of toluene using different beta zeolites (90 wt% $HNO_3$, $Ac_2O$, toluene/$HNO_3 = 1$, 30 min)

| | NT yield (mol%) | DNT yield (mol%) | $S_{2\text{-NT}}$ (mol%) | $S_{4\text{-NT}}$ (mol%) |
|---|---|---|---|---|
| H-PB1 | 84 | 0.4 | 36 | 61 |
| H-PB3 | 83 | 1.0 | 37 | 61 |
| H-PB5 | 76 | 1.4 | 26 | 72 |
| H-PB13 | 80 | 0.9 | 37 | 61 |
| H-BEA-24 | 81 | 1.1 | 31 | 66 |
| H-BEA-150 | 81 | 2.9 | 24 | 74 |
| H-PQ | 75 | 2.2 | 25 | 72 |
| H-PQ[a] | 81 | 1.0 | 24 | 73 |
| H-PQ[b] | 77 | 2.3 | 22 | 75 |
| H-RAMB | 77 | 0.4 | 37 | 61 |
| H-RAHB | 74 | 0.2 | 46 | 57 |
| Si-Beta | 75 | 0.05 | 57 | 39 |

[a] 2nd Nitration run after regeneration at 550 °C during 10 h (1 °C/min heating rate).
[b] 3rd Nitration run after regeneration at 550 °C during 10 h (1 °C/min heating rate).

Table 5
Nitration of toluene using H-PB5 with 90 wt% $HNO_3$, $Ac_2O$, and toluene/$HNO_3 = 0.1$

| Time (h) | NT yield (mol%) | DNT yield (mol%) | $S_{2\text{-NT}}$ (mol%) | $S_{4\text{-NT}}$ (mol%) | $S_{2,4\text{-DNT}}$[a] (mol%) |
|---|---|---|---|---|---|
| 0.23 | 50 | 23 | 16 | 81 | 96 |
| 0.5 | 35 | 45 | 3 | 92 | 97 |
| 16.0 | 9.6 | 83 | 0 | 91 | 98 |

[a] $S_{2,4\text{-DNT}}$ is defined as (2,4-DNT/$\Sigma$DNT) $*$ 100.

Table 6
Product composition analyzed by dissolving the zeolite in 48 wt% HF after the reaction

| | | $S_{4\text{-NT}}$ (mol%) |
|---|---|---|
| BEA | Pores[a] | 69 |
| | Liquid phase[b] | 66 |
| ZSM-5 | Pores | 38 |
| | Liquid phase | 40 |
| USY | Pores | 42 |
| | Liquid phase | 38 |
| H-MOR(4.6) | Pores | –[c] |
| | Liquid phase | 39 |
| H-MOR(74) | Pores | 43 |
| | Liquid phase | 43 |

[a] Products retained inside of the pores.
[b] Products in the reaction mixture.
[c] No products detected inside the pores.

Table 7
Nitration of 2-NT using different catalysts (90 wt% $HNO_3$, $Ac_2O$, NT/$HNO_3 = 0.1$)

| | DNT yield (mol %) | | $S_{2,4\text{-DNT}}$[a] (mol%) | |
|---|---|---|---|---|
| | 30 min | 16 h | 30 min | 16 h |
| Blank | 0.2 | 3.4 | [b] | 56 |
| H-PB1 | 41 | 94 | 93 | 93 |
| H-PB5 | 90 | 100 | 94 | 94 |
| H-PB13 | 29 | 100 | 93 | 94 |
| H-BEA-24 | 34 | 96 | 93 | 93 |
| H-BEA-150 | 38 | 96 | 95 | 94 |
| H-PQ | 85 | 98 | 94 | 94 |
| H-RAMB | 20 | 90 | 94 | 93 |
| H-RAHB | 12 | 70 | 90 | 91 |
| H-MC-Beta | 3.4 | 24 | 80 | 81 |
| H-ZSM-5 | 1 | 7 | 60 | 61 |
| H-ZSM-12 | – | 14 | – | 64 |
| H-MOR(4.6) | 1 | 9 | 57 | 61 |
| H-MOR(74) | 9 | 25 | 78 | 79 |

[a] Mixed acid process: $S_{2,4\text{-DNT}}$ (from 2-NT) = 67%.
[b] Too low amounts for a reliable value.

selectivity, suggesting that 2-NT reacts faster to 2,4-DNT than 4-NT.

Since high yields were observed even without a solid acid catalyst and after a short reaction time (5 min), a significant contribution of the nonselective homogeneous reaction must be considered when interpreting the results with solid catalysts. This can mask the actual behavior of the solid acid, and the intrinsic 4-NT selectivity of the zeolite-catalyzed nitration might be much higher. In order to clarify this point the catalysts recovered after the reactions were treated with 48 wt% HF to destroy the zeolite framework and the products retained inside of the pores were analyzed. The results of the analysis (Table 6) show that, in the case of BEA, ZSM-5, and USY, the product composition is the same as in the liquid phase meaning that the products can easily diffuse through the pores. A notable difference in the product composition was observed for the two mordenite samples: no products were found inside the pores of H-MOR(4.6), whereas in the dealuminated sample H-MOR(74) products were observed inside the pores and the selectivity was the same both inside and outside the pores. This suggests that diffusion is very difficult in the untreated samples, probably due to the 1-dimensionality of the channel system, while after the thermal treatment and subsequent formation of a secondary mesoporous system toluene and nitrotoluene can freely diffuse inside the pores. Only BEA, however, displays an enhanced *para*-selectivity both in the liquid phase and inside the pores, suggesting a higher contribution of the heterogeneous catalyzed nitration over the homogeneous nonselective reaction. This idea is supported by the fact that in the blank reaction and in the reaction carried out with ZSM-5, USY, and mordenite, a considerable amount (0.5–1%) of $\alpha$-NT was detected, while this was not the case with BEA. The absence of this typical by-product of the homogeneous reaction in the case of BEA suggests that the heterogeneous catalyzed reaction dominates over the homogeneous reaction. For the other three zeolites, however, the heterogeneous reaction seems to be too slow to compete with the unselective homogeneous nitration.

### 3.2.2. Nitration of 2-nitrotoluene

Nitration of 2-NT was carried out under the same experimental conditions as for toluene. The results in Table 7 show that 2-NT reacted with a high selectivity to 2,4-DNT on all the beta zeolites and that the reaction did not end after 30 min (same time as for the nitration of toluene). After 16 h reaction time, the DNT yield increased substantially, while the 2,4-DNT selectivity remained essentially constant. The nitration of 2-NT was also carried out without a catalyst. In this case we observed low DNT yields, which means that the contribution of the homogeneous reaction is very small. The same trends in selectivity that were found in the nitration of toluene were also observed for the nitration of 2-NT. H-PB5 and H-PQ were the most active catalysts with a 2,4-DNT selectivity of 94%. Zeolites other than beta were only slightly active and not *para*-selective [29]. H-ZSM-12 gave a DNT yield of 14 mol% after 16 h nitration with a 2,4-DNT selectivity of 64%.

### 3.3. Stability of H-BEA

The stability of the beta zeolites was tested by means of a threefold nitration with intermediate regeneration in air at 550 °C (Table 4). The *para*-selectivity, which is more indicative of the contribution of the zeolite than the activity, increased slightly in the subsequent runs. $^{27}$Al solid-state MAS NMR showed a decrease in the octahedral extraframework aluminum after the subsequent runs (Table 8). Almost no extraframework aluminum was found after the three nitration runs. The bulk Si/Al ratio determined by AAS increased from 13 before nitration to 30 after the three nitration steps with intermediate regeneration. Quantitative $^{27}$Al MAS NMR showed that not only the extraframework Al

Table 8
Al content of H-PQ before and after nitration (F, framework; EF, extra-framework; $Al_{bulk} = 3.3\%$)

| | Before nitration | After 1 nitration | After 3 nitrations |
|---|---|---|---|
| $Al_F$[a] (mmol/g) | 0.99 | 1.09 | 0.55 |
| $Al_{EF}$[a] (mmol/g) | 0.23 | 0.13 | 0 |
| $(Si/Al)_{bulk}$[b] | 13 | – | 30 |
| $(Si/Al)_F$[c] | 16 | – | 30 |
| $(Si/Al)_F$[d] | 16 | 18 | 25 |

[a] From $^{27}$Al MAS NMR.
[b] From AAS.
[c] From combination of AAS and $^{27}$Al MAS NMR.
[d] From quantitative $^{27}$Al MAS NMR, using H-PQ before nitration as reference.

Table 9
Approximate smallest dimension (MIN-1) and second smallest dimension (MIN-2) of 2-NT, 4-NT, 2,4-DNT, 2,6-DNT, and their Wheland intermediates

| Molecules | MIN-1 (Å) | MIN-2 (Å) |
|---|---|---|
| 2-NT (Wheland intermediate) | 5.9 | 8.0 |
| 2-NT | 4.2 | 7.8 |
| 4-NT (Wheland intermediate) | 5.7 | 6.8 |
| 4-NT | 4.2 | 6.7 |
| 2,4-DNT (Wheland intermediate) | 5.9 | 8.0 |
| 2,4-DNT | 4.2 | 7.8 |
| 2,6-DNT (Wheland intermediate) | 5.9 | 8.3 |
| 2,6-DNT | 4.2 | 8.3 |

was removed during the nitration, but also that the framework Al content decreased. After three nitration steps only 64% of the original framework Al was found. The framework Si/Al ratio of 25, calculated from the quantitative $^{27}$Al MAS NMR of the sample after three nitration steps, is in reasonable agreement with that determined by AAS.

### *3.4. Molecular dimensions*

According to Webster et al. [30,31] a molecule can enter a cylindrical pore if the smaller dimension of the molecule (MIN-1) and the second smaller dimension of the molecule perpendicular to MIN-1 (MIN-2) are equal to or smaller than the pore diameter. Table 9 lists the approximate values of MIN-1 and MIN-2 of 2-NT, 4-NT, and 2,6-DNT and their corresponding Wheland intermediates calculated with HyperChem 5.01 using the semiempirical PM3/UHF method. These are approximate values because the minimal distances between the atoms (and not of the molecule) were calculated (including the van der Waals radii of the atoms, 1.2 Å for H and 1.4 Å for O [32]). The values slightly overestimate the minimal dimensions of the molecules. Due to the similar geometrical arrangement, the minimal dimensions of 2,4-DNT were assumed to be equal to those of 2-NT.

### *3.5. $^{15}$N NMR experiments*

The results of the $^{15}$N NMR experiments carried out on the impregnated zeolite samples are summarized in Table 10.

Table 10
$^{15}$N NMR—Linewidth (Hz) of the peaks after MAS and static experiment

| | BEA | H-MOR(74) | ZSM-5 | Liquid mixture |
|---|---|---|---|---|
| MAS ($HNO_3$) | 48 | 26 | 30 | – |
| Static ($HNO_3$) | 102 | 80 | 78 | 75 |
| MAS ($AcONO_2$) | 40 | 26 | 36 | – |
| Static ($AcONO_2$) | 110 | 76 | 68 | 24 |

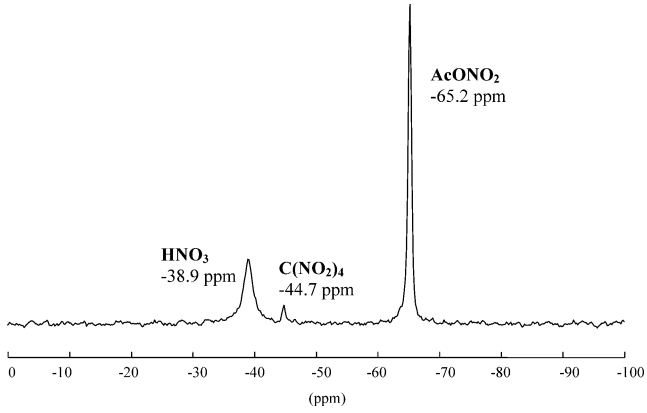


Fig. 4. $^{15}$N NMR spectrum of a 90 wt% $HNO_3$–$Ac_2O$ mixture with $HNO_3/Ac_2O$ ratio of 0.69.

Right after the sample was prepared a MAS experiment was carried out at 5 kHz. After this first experiment, a static NMR experiment was run under the same experimental conditions. For the sake of comparison, a spectrum of a mixture of $HNO_3$ and $Ac_2O$ ($HNO_3/Ac_2O = 0.69$) without a catalyst was also recorded (Fig. 4). In the liquid-state spectrum three peaks were observed at −65.2, −44.7, and −38.9 ppm, corresponding to acetyl nitrate, tetranitromethane (arising from the decomposition of $AcONO_2$), and nitric acid respectively [22].

In the static spectra of impregnated $HNO_3$, a linewidth of ∼80 Hz was observed for dealuminated mordenite (H-MOR(74)) and ZSM-5. This value is comparable to that measured in the liquid state (75 Hz). However, in case of BEA the observed linewidth was larger, which may indicate that the interaction of $HNO_3$ with the zeolite lattice is stronger.

For the acetyl nitrate we noticed that the reduction of the linewidth upon spinning and also the absolute width of the static spectra follow the order BEA > MOR > ZSM-5. This confirms the above conclusion, that BEA has a higher fraction of surface-bound species.

## 4. Discussion

The nitration of toluene with acetyl nitrate is a good model system for studying the enhanced *para*-selectivity of beta zeolites. It permits the use of mild reaction conditions without having to consider mediating effects of water

or thermally induced deactivation of the catalyst, as occurs during the vapor-phase nitration. One of the shortcomings, however, is the occurrence of the homogeneously catalyzed nitration, as is apparent from the high NT yields in the blank experiments. Therefore, the competition of the homogeneously catalyzed reaction for the formation of NT makes yields less meaningful. The 4-NT selectivities, however, reflect the relative contribution of the solid acid-catalyzed reaction to the formation of NT. For the more demanding conversion of NT to DNT, where very limited activity was observed in the experiments without catalyst, yields are a direct indication of the heterogeneous catalyzed nitration.

The enhanced 4-NT selectivity during toluene nitration is a unique property of BEA zeolites since none of the other catalysts showed a substantial increase in the formation of 4-NT. This trend was also observed in the case of the nitration of 2-NT (Table 7). In earlier experiments, a high yield of DNT was obtained when the nitration of toluene was carried out with varying excess of nitric acid [8], with the main product being 2,4-DNT. During these experiments it was observed that the selectivity to the intermediate product 4-NT increased with increasing $HNO_3$/toluene ratio, which indicated the preferential reaction of the intermediate 2-NT to DNT. The results of the time-on-stream study (Table 5) give a similar picture. Using the 2,4-DNT and 2,6-DNT selectivities obtained in the nitration of 2-NT (Table 7), we determined the amount of DNT that originates from 2-NT and 4-NT in the dinitration of toluene. Since 2,6-DNT can only be formed by nitration of 2-NT and the selectivity to 2,4-DNT vs 2,6-DNT in the nitration of 2-NT is known (Table 6), the amount of DNT formed from 2-NT ($(DNT)_{2\text{-NT}}$) can be calculated by $(DNT)_{2\text{-NT}} = 2{,}6\text{-DNT}/(1 - S_{2,4\text{-DNT}})$. The amount of DNT formed from 4-NT ($(DNT)_{4\text{-NT}}$) is then simply obtained by $(DNT)_{4\text{-NT}} = (DNT)_{tot} - (DNT)_{2\text{-NT}}$. The results are shown in Fig. 5. The total 4-NT/2-NT product ratio did not change with reaction time and was identical to that obtained in experiments with a $HNO_3$/toluene ratio of 1. This suggests that the selectivity in the first nitration step is an intrinsic property of beta zeolites.

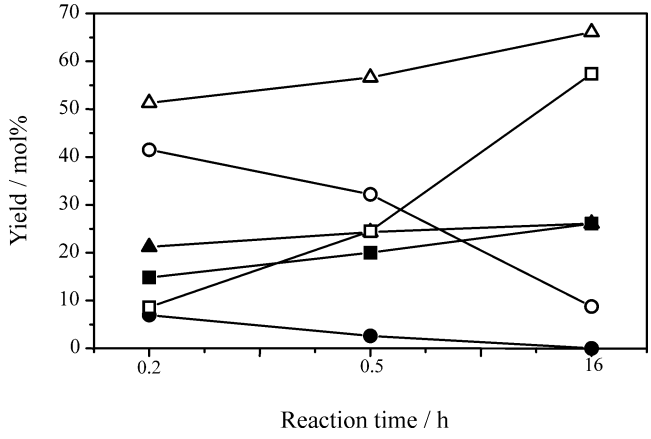


Fig. 5. Nitration of toluene with H-PB5 ($T/HNO_3 = 0.1$). Total amount of 2-NT (▲) and of 4-NT (△), amount of 2-NT (●) and 4-NT (○) that was observed as isolable product and amount of 2-NT (■) and 4-NT (□) that had reacted to DNT.

In situ infrared measurements of the adsorption of 2-NT and 4-NT showed that all the acid sites were rapidly covered after the exposure of H-beta to 10 Pa NT [29]. This confirmed that this zeolite, having pore openings of $7.6 \times 6.4$ Å, will not impose steric restrictions to the penetration of nitrotoluenes.

The analysis of the products retained inside the pores, performed by dissolving the zeolite with 48 wt% HF, revealed that, in case of USY, ZSM-5, and BEA, the products easily diffuse through the pores, suggesting the absence of diffusion limitations. The quantification and comparison of the product composition (Table 6) showed that, in the case of BEA, an increased selectivity is observed both inside the pores and in the liquid phase, indicating that the heterogeneous catalyzed nitration dominates over the homogeneous reaction. This result is confirmed by the fact that $\alpha$-NT, which is observed in the reaction without a catalyst and is therefore assumed to arise from the homogeneous reaction, was not detected in the reaction carried out with BEA. On the other hand, for USY, ZSM-5, and the dealuminated MOR, the *para*-selectivity inside the pores is similar to that observed in the liquid phase. This suggested two possible explanations: (1) the reaction does not take place inside the pores and (2) the heterogeneous reaction inside the pores does not induce an enhanced *para*-selectivity. The latter interpretation was ruled out by the fact that, in the reaction with these zeolites, the secondary product $\alpha$-NT was observed in the same amounts as in the blank reaction, indicating that the heterogeneous reaction is not fast enough to compete with the homogeneous reaction.

Nitration is an irreversible reaction; thus, reequilibration of 2-NT to 4-NT cannot be the cause for the enhanced selectivity observed [6]. This leads to the obvious suggestion that transition-state selectivity may be invoked to explain the high *para*-selectivity. From Table 9 it is inferred that the critical transition state, i.e., the Wheland intermediate, is comparable in size to the product molecules. Therefore a severe restriction of the formation of the Wheland intermediate, which leads to the formation of 2-NT, should also be manifested in a consequential blockage of the adsorption of 2-NT. This was, however, not the case [29]. The steric requirements for the nitration of toluene and for the nitration of 2-NT are considerably different. Thus, if transition-state selectivity governed the enhanced formation of 4-NT from toluene, further nitration to DNT would not be possible. It is therefore concluded that classical transition-state selectivity does not explain the observed results.

In recent communications, NMR measurements proved the contribution of the surface-catalyzed reaction on beta zeolites to the enhanced *para*-selectivity and linked it to the presence of flexible lattice aluminum species, that change coordination upon $HNO_3$ adsorption [22,33]. It was proposed that the arene reacts with a preadsorbed reactive nitrating species (acetyl nitrate) and forms the sterically least

hindered Wheland intermediate, and that the reaction products finally desorb. In the case of toluene adsorption, the Wheland intermediate leading to 4-NT should form preferentially because the methyl group would point toward the zeolite cavity and would be repelled by the zeolite lattice to a lesser extent. In the case of 2-NT adsorption, the Wheland intermediate, which leads to 2,4-DNT, should form preferentially because this will orient the methyl and the nitro group toward the zeolite cavity. On the other hand, adsorption of 4-NT on the preadsorbed reactive nitrating species will always result in a less favorable arrangement for the Wheland intermediate due to the methyl group being close to the zeolite lattice. This is in line with the higher reactivity of 2-NT compared to 4-NT for further nitration and with the high 2,4-DNT selectivity observed. The model also explains the absence of *para*-selectivity in the case of Si-Beta, where the nitrating agent cannot coordinate to the zeolite framework.

To test the validity of the proposed model and to ascertain whether $AcONO_2$ is bound to the surface to a different extent, depending on the zeolite used, the $^{15}N$ NMR of a mixture of nitric acid and acetic anhydride adsorbed on the catalysts in MAS, and static conditions was measured. The experiment was carried out using three different catalysts: BEA, dealuminated MOR (H-MOR(74)), and ZSM-5. It is known that the NMR spectra of solids suffer from broadening due to dipole–dipole interaction and chemical-shift anisotropy [34].

In the case of adsorbed acetyl nitrate, a dipolar interaction (direct coupling of two spins, magnetic dipoles) is possible with the Al to which $AcONO_2$ is bound. The next proton is quite far; dipolar coupling should therefore be weak. This argument was confirmed by our previous work [22], where $^{15}N\{^1H\}$ CP-MAS failed to reveal any signals, indicating that an efficient cross-polarization from proton to nitrogen did not occur. Due to the angular dependence $(3\cos^2\theta - 1)$, the line broadening caused by dipolar interactions is reduced to zero by magic-angle spinning ($\cos\theta = 1/\sqrt{3}$).

The chemical-shift anisotropy is caused by the noncentrosymmetric shielding effect of the surrounding electrons and is described by

$$\sigma_{zz} = \sigma + \tfrac{1}{2}\delta_{CS}\big[\big(3\cos^2\theta - 1\big) + \eta_{CS}\big(\sin^2\theta\cos 2\phi\big)\big], \quad (1)$$

where $\sigma$ is the chemical shielding ($\sigma_{zz} = zz$ component), $\delta_{CS}$ the anisotropy parameter, and $\eta_{CS}$ the asymmetry parameter.

$$\sigma = \tfrac{1}{3}\big(\sigma_{xx} + \sigma_{yy} + \sigma_{zz}\big), \quad (2)$$

$$\delta_{CS} = \sigma_{zz} - \sigma, \quad (3)$$

$$\eta_{CS} = \frac{\sigma_{xx} - \sigma_{yy}}{\sigma_{zz} - \sigma}. \quad (4)$$

If $\eta_{CS} = 0$, then the chemical-shift anisotropy is also averaged by magic-angle spinning. In the case of acetyl nitrate, there is a symmetry axis and the chemical-shift anisotropy should therefore be removed. However, if $\eta_{CS} \neq 0$, then a time-dependent part remains in the Hamiltonian, which is only averaged at fast spinning rates, i.e., when the spinning is much faster than the line broadening. The spinning frequency in our experiment was only 5 kHz, which is probably not sufficient to average out the time-dependent part.

Table 10 shows the linewidth of the peaks of $HNO_3$ and $AcONO_2$ of the three zeolites and of a liquid mixture of $HNO_3$ and $Ac_2O$. In the static spectra of $HNO_3$, the linewidth was 80 Hz for MOR and ZSM-5, whereas it was 100 Hz for BEA. The linewidth observed in the liquid spectrum was comparable to the values of MOR and ZSM-5, suggesting that $HNO_3$ is essentially in a liquid state. The quite high value for the linewidth measured even in the liquid sample may be due to a distribution of the chemical shifts of $HNO_3$ caused by the strong hydrogen bond $O_2N$–$OH\cdots O_2N$–OH. Hydrogen bonding affects the shielding of the nitrogen nucleus and, thus, its chemical shift. The greater linewidth of BEA may indicate that, in this case, an interaction of $HNO_3$ with the zeolite lattice occurred.

Acetyl nitrate has a lower tendency to form hydrogen bonds than $HNO_3$. This explains why the linewidth of $AcONO_2$ in the liquid spectrum was smaller than that of $HNO_3$. In all three zeolites, however, the linewidth of $AcONO_2$ increased strongly compared to the liquid phase. Three factors contribute to this line broadening: (i) a distribution of the chemical shift caused by interaction of the $–NO_2$ group with lattice aluminum, (ii) dipolar interactions with lattice aluminum, and (iii) the chemical-shift anisotropy of surface-bound $AcONO_2$, which cannot be averaged out by molecular motions any more. The linewidth of the static spectrum can, therefore, be taken as a measure of the degree of interaction of the $AcONO_2$ with the zeolite lattice. It increased in the order ZSM-5 < MOR < BEA. Magic-angle spinning removes the contribution of dipolar interactions and of chemical-shift anisotropy to the linewidth (vide supra). The decrease in linewidth, caused by magic-angle spinning, is a second indicator of the portion of surface-bound species. It followed the same order as the absolute linewidth of the static spectrum, i.e., ZSM-5 < MOR < BEA.

The residual linewidth of the MAS spectrum is due mainly to chemical-shift distributions induced by the interaction of $AcONO_2$ with the lattice aluminum. Furthermore, the line broadening due to chemical-shift anisotropy remains in the MAS spectrum if the symmetry of the $–ONO_2$ group is distorted ($\eta_{CS} > 0$). Asymmetry in the $–ONO_2$ group can be induced by interaction with the pore, for example, in a surface-bound complex as shown in Fig. 6. The relatively strong interaction of BEA with $AcONO_2$ is, thus, also responsible for the large residual linewidth in the MAS spectrum.

A large residual linewidth was also found in the MAS spectrum of ZSM-5, in contrast to our assumption that ZSM-5 hardly interacts with $AcONO_2$. The effect is ascribed to the spatial constraints induced by the 10-membered ring pores of $AcONO_2$, which may cause a distortion of the $AcONO_2$ molecules and render $\eta_{CS} > 0$.

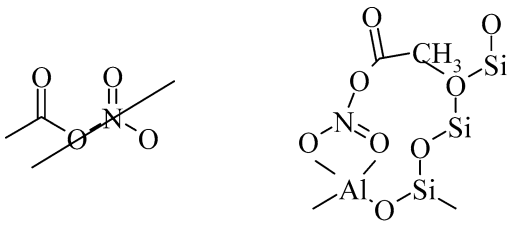

Fig. 6. Scheme for the proposed distortion of the $NO_2$ group caused by the interaction with the zeolite lattice.

## 5. Conclusion

The nitration of toluene in the liquid phase with acetic anhydride and nitric acid demonstrated that, when an equimolar amount of the nitrating agent is used, a high selectivity to 4-NT can be obtained only with zeolite beta. The results of this study show that the reaction takes place inside the pores of BEA. Only with beta zeolite the heterogeneous catalyzed nitration competes effectively with the homogeneous reaction. Using 2-NT as the reactant, the selectivity toward 2,4-DNT was exceptionally high.

Semiempirical calculations of the sizes of the transition states (the Wheland intermediates) showed that they are about the same size as the reaction products. These and earlier results of in situ IR adsorption experiments suggest that the high *para*-selectivity of BEA is not caused by classical transition-state selectivity, i.e., spatial constrictions within the zeolite cage. The reaction with a surface-bound acetyl nitrate complex induces steric hindrance and directs the formation of the Wheland intermediate.

Our $^{15}N$ NMR studies show that a large portion of this surface-bound acetyl nitrate is present only on zeolite BEA and explain why a high *para*-selectivity is found exclusively with this zeolite.

## Acknowledgments

We are indebted to Dr. M. Haouas and A. Abraham for their assistance in performing the NMR experiments.

## References

[1] C.K. Ingold, Structure and Mechanism in Organic Chemistry, Cornell Univ. Press, New York, 1969.
[2] K. Schofield, Aromatic Nitration, Cambridge Univ. Press, Cambridge, 1980.
[3] G.A. Olah, R. Malhotra, S.C. Narang, Nitration Methods and Mechanisms, Chemie, New York, 1989.
[4] L.V. Malysheva, E.A. Paukshtis, K.G. Ione, Catal. Rev.-Sci. Eng. 37 (1995) 179.
[5] A. Kogelbauer, H.W. Kouwenhoven, in: R.A. Sheldon, H. van Bekkum (Eds.), Fine Chemicals through Heterogeneous Catalysis, Wiley–VCH, Weinheim, 2000, p. 213.
[6] A. Germain, T. Akouz, F. Figueras, J. Catal. 147 (1994) 163.
[7] J.M. Smith, H. Liu, D.E. Resasco, Stud. Surf. Sci. Catal. 111 (1997) 199.
[8] D. Vassena, A. Kogelbauer, R. Prins, Stud. Surf. Sci. Catal. 125 (1999) 501.
[9] R.P. Claridge, N.L. Lancaster, R.W. Millar, R.B. Moodie, J.P.B. Sandall, J. Chem. Soc., Perkin Trans. 2 (1999) 1815.
[10] B.M. Choudary, M. Sateesh, M. Lakshmi Kantam, K. Koteswara Rao, K.V. Ram Prasad, K.V. Raghavan, J.A.R.P. Sarma, Chem. Commun. (2000) 25.
[11] T.J. Kwok, K. Jayasuriya, R. Damavarapu, B.W. Brodman, J. Org. Chem. 59 (1994) 4939.
[12] S.M. Nagy, K.A. Yarovoy, V.G. Shubin, L.A. Vostrikova, J. Phys. Org. Chem. 7 (1994) 385.
[13] K. Smith, A. Musson, G.A. DeBoos, J. Org. Chem. 63 (1998) 8448.
[14] L. Delaude, P. Laszlo, K. Smith, Acc. Chem. Res. 26 (1993) 607.
[15] O.L. Wright, J. Teipel, D. Thoennes, J. Org. Chem. 30 (1965) 1301.
[16] H. Schubert, F. Wunder, Process for nitrating toluene, US patent 4'112'006, 1978.
[17] A. Kogelbauer, D. Vassena, R. Prins, J.N. Armor, Catal. Today 55 (2000) 151.
[18] D.B. Akolekar, G. Lemay, A. Sayari, S. Kaliaguine, Res. Chem. Intermed. 21 (1995) 7.
[19] F.J. Waller, A.G.M. Barrett, D.C. Braddock, D. Ramprasad, Chem. Commun. (1997) 613.
[20] F.J. Waller, A.G.M. Barrett, D.C. Braddock, D. Ramprasad, Tetrahedron Lett. 39 (1998) 1641.
[21] K. Smith, A. Musson, G.A. DeBoos, Chem. Commun. (1996) 469.
[22] M. Haouas, S. Bernasconi, A. Kogelbauer, R. Prins, Phys. Chem. Chem. Phys. 3 (2001) 5067.
[23] M.A. Camblor, A. Corma, S. Valencia, Chem. Commun. (1996) 2365.
[24] L. Bertea, H.W. Kouwenhoven, R. Prins, Appl. Catal. A 129 (1995) 229.
[25] B.C. Lippens, J.H. de Boer, J. Catal. 4 (1965) 319.
[26] E.P. Barret, L.G. Joyner, P.P. Halenda, J. Am. Chem. Soc. 73 (1951) 373.
[27] M.A. Harmer, W.E. Farneth, Q. Sun, J. Am. Chem. Soc. 118 (1996) 7708.
[28] D. Vassena, A. Kogelbauer, R. Prins, Catal. Today 60 (2000) 275.
[29] D. Vassena, A. Kogelbauer, R. Prins, Stud. Surf. Sci. Catal. 130 (2000) 515.
[30] C.E. Webster, R.S. Drago, M.C. Zerner, J. Am. Chem. Soc. 120 (1998) 5509.
[31] C.E. Webster, R.S. Drago, M.C. Zerner, J. Phys. Chem. B 103 (1999) 1242.
[32] R.C. Weast, Handbook of Chemistry and Physics, The Chemical Rubber, Cleveland, 1970.
[33] M. Haouas, A. Kogelbauer, R. Prins, Catal. Lett. 70 (2000) 61.
[34] G. Engelhardt, D. Michel, High Resolution Solid-State NMR of Silicates and Zeolites, Wiley, Chichester, 1987.